X-ray and neutron studies on muon to alpha sticking in D-T muon catalyzed fusion

Katsuhiko Ishida,*1 Kanetada Nagamine,*1,*2,*3 Teiichiro Matsuzaki,*1 Satoshi N. Nakamura,*1 Naritoshi Kawamura,*1,*2,*3 Shinichi Sakamoto,*2,*3 Masahiko Iwasaki,*3,† Isao Watanabe,*1 Masakazu Tanase,*4 Mineo Kato,*4 Kiyoyuki Kurosawa,*4 Katsuhisa Kudo,*5 Naoto Takeda,*5 and Gordon H. Eaton*6

*1 *Muon Science Laboratory, RIKEN*
*2 *Meson Science Laboratory, Institute of Materials Structure Science, High Energy Accelerator Research Organization (KEK-MSL)*
*3 *Meson Science Laboratory, Faculty of Science, University of Tokyo (UT-MSL)*
*4 *Department of Radioisotopes, Japan Atomic Energy Research Institute (JAERI)*
*5 *Quantum Radiation Division, Electrotechnical Laboratory (ETL)*
*6 *ISIS Muon Facility, Rutherford Appleton Laboratory (RAL), UK*

Precise measurements of the absolute yields and the disappearance rates were carried out both for the X-rays from $(\alpha\mu)^+$ ion formed by muon to alpha sticking after the muon catalyzed fusion and for the fusion neutrons from ^{3}He-free liquid and solid $D_{1-x}T_x$ mixture with $x = 0.10$, 0.20, 0.28, 0.40, 0.50, 0.60 and 0.70. While the $\alpha\mu$ X-ray yield is not contradicting with some of the values predicted by the atomic-process theories, the effective sticking probability ω_s obtained by neutron measurement is much smaller than any of the calculations published so far, suggesting *e.g.* enhanced reactivation.

Introduction

The muon to alpha sticking probability (ω_s) is one of the most important observables in all the muon catalyzed fusion (μCF) studies (Fig. 1); the ω_s limits stringently the energy-production capability from μCF[1-3] as it is the main component of the muon loss. In order to investigate the basic properties of the μCF phenomena in D-T mixture, various experimental methods can be applied. So far, most of the experiments on D-T μCF conducted at Los Alamos and PSI in 1980's have focused on neutron measurements.[4,5] From the measurement of the neutron disappearance rate λ_n ($= \lambda_0 + W\phi\lambda_c$) and the fusion neutron yield Y_n ($= \phi\lambda_c/\lambda_n$), the cycling rate λ_c and the muon loss probability W per cycle can be obtained. Here ϕ is the density of D-T mixture normalized to the liquid hydrogen density, and λ_0 is the free muon decay rate. The ω_s is obtained by subtracting other contributions from W such as muon sticking through $dd\mu$ and $tt\mu$ formation and muon transfer to impurity atoms such as ^{3}He.

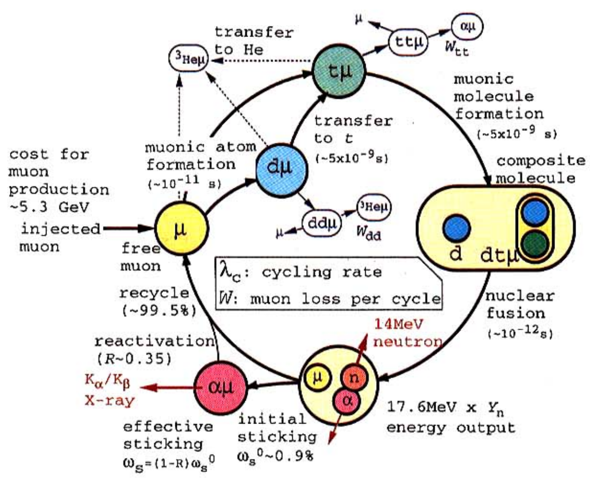

Fig. 1. Simplified diagram of the muon catalyzed fusion cycle.

However, there has been a great puzzle in the value of ω_s; the ω_s determined from W has been always smaller than the theoretically predicted ω_s which is calculated as $(1-R)\omega_s^0$, where ω_s^0 is the initial sticking probability right after the dt-fusion and R is the muon reactivation probability due to the ionization or transfer of muons from the energetic $(\alpha\mu)^+$.

Concerning this problem, the characteristic X-rays can give us valuable insights about the atomic process of $(\alpha\mu)^+$ ions. For the K_α X-ray, a central energy of 8.2 keV with a Doppler broadening of 0.5 keV FWHM are expected.[6] The K_α X-ray yield is given as $Y(K_\alpha) = \gamma_{K_\alpha}\omega_s^0$, where γ_{K_α} is the number of X-rays emitted per $(\alpha\mu)^+$ ion and can be calculated by the same atomic process calculation as used for R.

However, the X-ray measurement in a high-density and high-C_t D-T mixture has been very difficult due to a huge radiation background of bremsstrahlung from tritium β decay (up to 17 keV); over 2×10^4 background photons/s were detected by our detection and target sytem described below. The help of pulsed muons is significant here, because the signal to noise ratio can be drastically increased by operating the X-ray detection only during the existence of the muon pulse. This type of experiment with pulsed muon beam had already been carried out by the UTMSL-RIKEN-JAERI collabora-

† Present address: Department of Physics, Tokyo Institute of Technology

tion at UTMSL/KEK.[7,8] There, the successful observation of the 8.2-keV K_α X-ray with a correct Doppler broadening was made for μCF in a liquid $D_{0.70}$-$T_{0.30}$ mixture. A similar experiment had been carried out at PSI with continuous muon beam only for a substantially low-C_t (4×10^{-4}) D-T mixture.[9] Now, with the help of the intense pulsed muon beam which has become available at RIKEN-RAL, we carried out systematic neutron and X-ray combined measurement for the first time.

Measurement

At the recently completed RIKEN-RAL muon facility,[10] the world-strongest pulsed negative muon beam is available from the superconducting muon channel (Fig. 2) installed at 800 MeV proton synchrotron, ISIS, of the Rutherford Appleton Laboratory, UK. There, the dedicated μCF experimental set-up was installed at one of the three experimental ports (Port 1). The essential part of the experimental arrangement is schematically depicted in Fig. 3. The advanced features of the present experiment are summarized as follows: (1) use of intense pulsed μ^- beam against a huge bremsstrahlung-background, where 70 muons with 54.5 MeV/c momentum were stopped in 1 cc liquid/solid D-T (1.2 $\sim$ 1.5 $\times$ liquid H_2 density) per double pulse (each 70 ns width with a 320 ns separation and 50 Hz) at the proton current of 200 μA. (2) ^{3}He-free D-T target was prepared by an advanced tritium handling system with *in-situ* ^{3}He removal and chemical composition analysis capabilities,[11] so that the data for zero ^{3}He concentration were obtained by an interpolation of the linearly increasing ^{3}He accumulation effect from the time-dependent data.

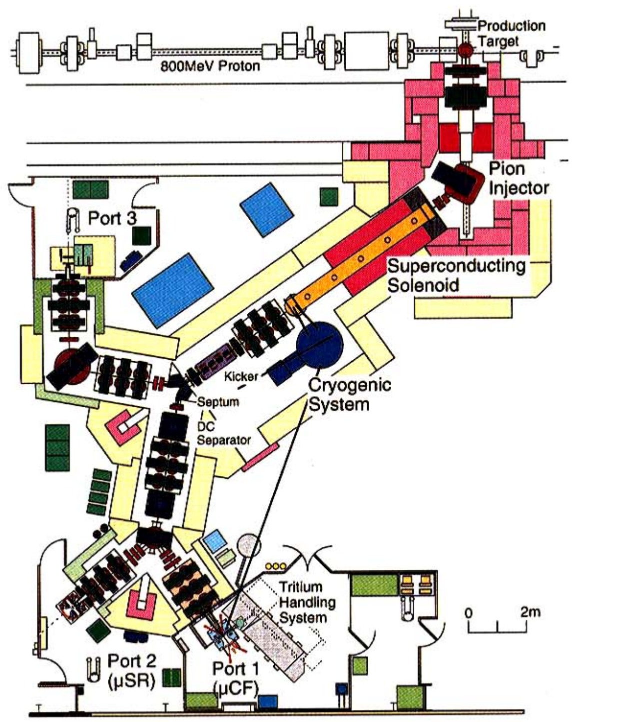

Fig. 2. Layout of the RIKEN-RAL Muon Facility. Pions produced by 800 MeV proton hitting the production target are collected by pion injector and decay into muons in the superconducting solenoid. The muons are delivered to three experimental ports. The muon catalyzed fusion experiment was carried out at Port 1, where an advanced tritium handling system was installed.

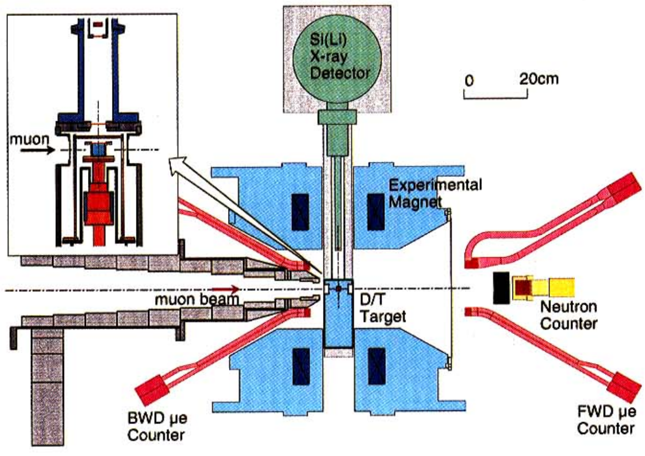

Fig. 3. Schematical figure of the present experiment (horizontal view). D-T target and X-ray/neutron/electron counters can be seen. The confinement magnetic field was applied along the incoming muon beam.

All the measurements were carried out by using 2.4 T confinement field for an enhanced focusing of μ^- beam onto 1 cc target and a confinement of decay e^- away from the X-ray detector. As shown in Fig. 3, we used an X-ray detector (Si(Li), 70 mm^2 $\times$ 3.5 mm thickness) placed at 13.3 cm from the target perpendicular to the μ^- beam. Also two neutron detectors (liquid scintillator NE213, 2" diameter and 2" length) were placed at 84 cm from the target along the μ^- beam and just behind a 5 cm thick Pb absorber. The neutron detecter efficiency was calibrated[12] by using 14 MeV neutrons at ETL(Tsukuba, Japan), and the X-ray detector efficiency was measured by using various calibrated sources. X-rays from the D-T target penetrated two 0.5 mm thick beryllium windows before reaching the Si(Li) detector. The μ^- stopping number in the D-T mixture was determined by using muonic X-rays and decay e^- from the beryllium window just beside the D-T mixture, where the μBe X-ray intensity was converted to the μ^- stopping number with a normalization by a difference in decay e^- intensities from D-T mixture versus beryllium. The D-T target status of either liquid or solid phase was monitored by measuring temperature and vapour pressure of the mixture. Advanced data-taking system was installed with logic electronics for counting loss estimation.[13]

Result

Typical X-ray spectra (within the time gate of 0.08-2.08 μs) are shown in Fig. 4. There, for each spectrum, a clear Doppler broadened $K_\alpha(n = 2 \rightarrow n = 1)$ peak from recoiling $(\alpha\mu)^+$ was seen at 8.2 keV well above bremsstrahlung background. At the same time, $K_\beta(n = 3 \rightarrow n = 1)$ line can be seen but with much reduced intensity. The disappearance rate of the K_α peak was also determined and was consistent with λ_n. The measured number of X-ray events was converted to the

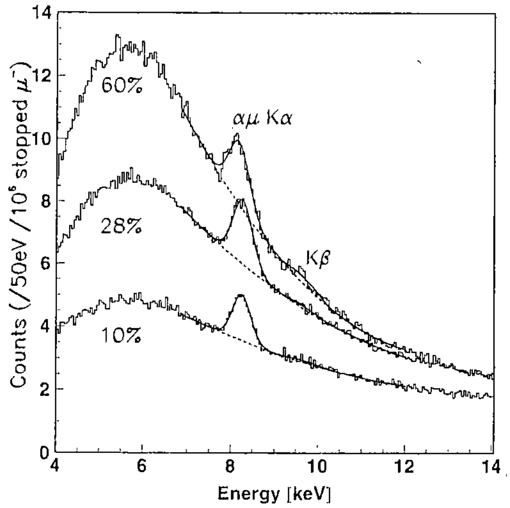

Fig. 4. Typical X-ray energy spectra from liquid D-T mixture with C_t = 10, 28 and 60% in the time range from 80 to 2080 ns after muon stopping.

X-ray yield after correcting multi-hit loss, counter efficiency, solid angle, attenuation through windows, and magnetic field effect. Similarly, the fusion neutron yield was obtained by correcting multi-hit loss, pile-up loss, counter efficiency, solid angle, and attenuation through target-chamber wall plus Pb absorber.

The values of λ_c obtained by neutron measurement are summarized in Fig. 5. In a series of measurements where we deliberately changed the target gas quantity, we observed a target quantity dependence of λ_n whose effect scaled roughly with the inverse of the target quantity. This may come from the muons near the target wall diffusing to the wall and being lost, although we do not have definite evidence yet. The correction resulted in reducing both λ_c and W by about 5% from the raw measured values.

Our λ_c values agree well with those of LAMPF[4,14] and PSI[15] at low concentrations but seems larger than "equilibrated" values[14,15] at high concentrations ($C_t \geq 0.4$). Although this kind of enhancement can come from non-equilibrium effect

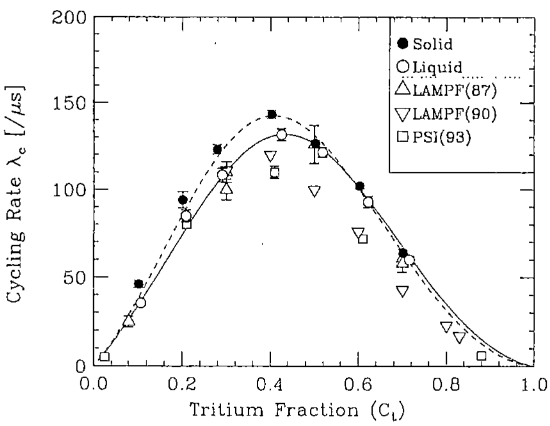

Fig. 5. The C_t dependence of the observed cycling rate λ_c for μCF in solid and liquid D-T mixture. The liquid data at LAMPF[4,15] and PSI[16] are also shown.

of molecular composition ($D_2/DT/T_2$),[1] it is hard to believe that our target was not in molecular equilibrium after the D-T gas mixture had passed through the palladium filter.

The cycling rate λ_c was analysed according to the formula considering the time spent in $d\mu$, $t\mu$-triplet and -singlet states[1]

$$\lambda_c = [q_{1s}C_d/(\lambda_{dt}C_t) + \frac{3}{4}/(\lambda_{t\mu}^{10}C_t) + 1/(\lambda_{dt\mu}^{0}C_d)]^{-1}, \quad (1)$$

where q_{1s} is the probability for the $d\mu$ to reach the ground state before transferring to t, and was parameterized as $q_{1s} = 1/(1 + a_q C_t)$. The $C_d (= 1 - C_t)$ is the deuterium fraction, λ_{dt} ($= 280\ \mu s^{-1}$)[16] is the muon transfer rate from the ground state of $d\mu$ to t, $\lambda_{t\mu}^{10}$ ($= 1300\ \mu s^{-1}$)[17] is triplet to singlet conversion rate, and $\lambda_{dt\mu}^{F}$ ($= \lambda_{dt\mu}^{F,D_2} C_d + \lambda_{dt\mu}^{F,DT} C_t$) is the $dt\mu$ formation from each hyperfine state (F) of $t\mu$ statistically averaged over collisions with D_2 and DT molecule. The $dt\mu$ formation from $t\mu$-triplet state was neglected at low temperatures.

The results of muon loss W and K_α X-ray yield Y_X/Y_n per fusion are shown in Fig. 6. One can consider the content of the possible other loss processes than ω_s in W following the arguments given by the references.[1,4] Experimentally, the D-T mixture in the present experiment is known to have only small amount of protium ($C_p \leq 0.1\%$). Concerning the ^{3}He

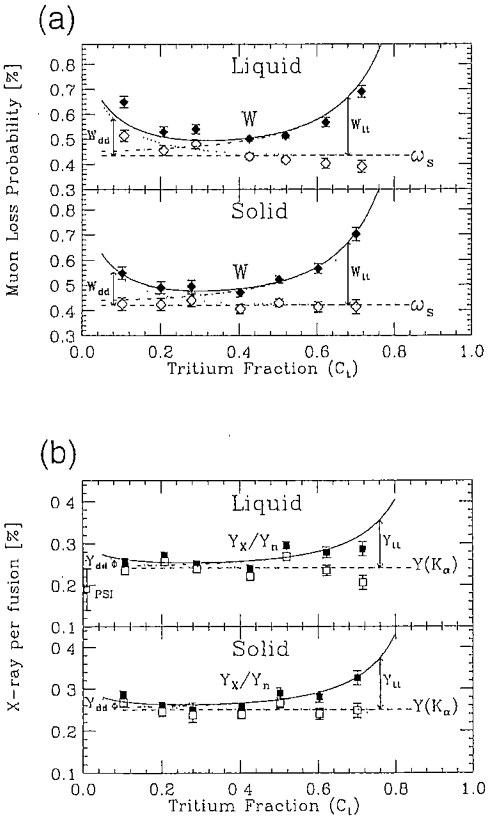

Fig. 6. (a) The total loss rate, W, obtained from the neutron data in solid and liquid D-T mixture, where the filled symbols are measured values and the lines are the result of fitting. The values of the effective sticking probability ω_s (open symbols) obtained by the subtractions of W_{dd} and W_{tt} described in the text and its average (dashed line) are also shown. (b) The K_α X-ray yield from $\alpha\mu$ per fusion (Y_X/Y_n, filled symbols) and the corrected values ($Y(K_\alpha)$, open symbols).

accumulation effect, as described in detail separately,[18] it was found that the effect is not significant at all in liquid phase but is totally significant in solid phase. As for the solid-phase data, all the results shown in Figs. 5 and 6 are already interpolated to zero ^{3}He concentration. Thus, significant remaining loss processes appearing in W are due to dd μCF and tt μCF.

$$W - \omega_s = W_{dd} + W_{tt}, \tag{2}$$

$$W_{dd} = \frac{2}{3} q_{1s} C_d \frac{\beta_d \lambda^{3/2}_{dd\mu} {C_d}^2 \omega_d}{\lambda_{dt} C_t + \lambda^{3/2,1/2}_{d\mu} C_d + \lambda^{3/2}_{dd\mu} {C_d}^2}, \tag{3}$$

$$W_{tt} = \lambda_{tt\mu} C_t \omega_t / (\lambda^0_{dt\mu} C_d), \tag{4}$$

where $\beta_d = 0.58$ is the ^{3}He+n fraction following dd-fusion, $\lambda^{3/2,1/2}_{d\mu}$ ($= 31\ \mu s^{-1}$)[19,20] is the $d\mu$ hyperfine transition rate, and $\lambda^{3/2}_{dd\mu}$ ($= 2.9\ \mu s^{-1}$)[19,20] is the $dd\mu$ formation rate from $d\mu$-quartet state both in solid D_2. We neglected $dd\mu$ formation from $d\mu$-doublet state, since it is much slower than the competitive rate λ_{dt} at low temperatures.[1] Also, $\lambda_{tt\mu}$ is the $tt\mu$ formation rate, averaged over hyperfine states and molecular composition, and ω_d and ω_t are muon sticking probabilities to ^{3}He in $dd\mu$ and ^{4}He in $tt\mu$ respectively. There, $\omega_d = 0.12$[1] and $\lambda_{tt\mu}\omega_t = 0.27 (\mu s^{-1})$ [21] are additionally assumed. The fitted values of the parameters (q_{1s} and $\lambda^0_{dt\mu}$) in Eq. (1) were used to estimate each term of Eqs. (2)–(4). The obtained ω_s, after subtraction of W_{dd} and W_{tt} from W, is shown in Fig. 6. It is almost C_t independent and the average gives values of ω_s ~0.43% for both solid and liquid.

The $Y(K_\alpha)$ can be obtained by taking the ratio of X-ray and neutron yields, Y_X and Y_n. Actually, Y_X has, like W, contributions from $dd-$ and $tt-\mu$CF; $Y_X/Y_n = Y(K_\alpha) + Y_{dd}(K_\alpha) + Y_{tt}(K_\alpha)$, where $Y_a(K_\alpha) = \gamma_{K_\alpha}(a) W_a / (1 - R_a)$; $(a = dd, tt)$. Here $\gamma_{K_\alpha}(a)$ and R_a are X-ray yield per initial sticking and reactivation probability, respectively. The $\gamma_{K_\alpha}(tt)/(1 - R_{tt})$ was recently measured by our group to be around 0.27[21] and was fixed in the analysis. As shown in Fig. 6(b), the $Y(K_\alpha)$ is obtained to be 0.25% for both solid and liquid case.

The obtained values of ω_s and $Y(K_\alpha)$ as well as the K_β/K_α X-ray intensity ratio $Y(K_\beta)/Y(K_\alpha)$ are summarized in Table 1. Our ω_s values were consistent with those of previous measurements, and confirmed again the gap between the experiments and the theory. Our results on $Y(K_\alpha)$ are not far away from the previous experiment on $Y(K_\alpha)$ at very low C_t,[9] but extended the X-ray results to various and higher C_t with high precision. In addition, the K_β/K_α intensity ratio was obtained for the first time.

Table 1. Effective sticking probability (ω_S), $\alpha\mu$ X-ray yield per dt-fusion ($Y(K_\alpha)$) and $Y(K_\beta)/Y(K_\alpha)$.

	ω_s (%)	$Y(K_\alpha)$(%)	$Y(K_\beta)/Y(K_\alpha)$
LAMPF[22]	0.43±0.05±0.06		
PSI[5]	0.45±0.05		
PSI[23]	0.48±0.02±0.04		
PSI[9]		0.19±0.05 (C_t=0.0004)	≤0.08
Present (Liquid)	0.434±0.030	0.242±0.017 (C_t=0.1~0.7)	0.075±0.010
Present (Solid)	0.421±0.030	0.250±0.017 (C_t=0.1~0.7)	0.060±0.012

Discussion

Our result can be compared with the atomic process calculation once the initial sticking probability is assumed. Figure 7 shows the values of ω_s and $Y(K_\alpha)$. Our experimental results can be compared with the values[24-27] corresponding to the theoretical estimate of initial sticking probability $\omega^0_s = 0.912\%$,[28] which are shown by the symbols. While the $\alpha\mu$ X-ray yield from our measurement is not contradicting with some of the values predicted by the atomic-process theories[24,25] with realistic Stark mixing at $n = 3$, the effective sticking probability ω_s obtained by neutron measurement is much smaller than any of the calculations published so far. In addition, the measured $Y(K_\beta)/Y(K_\alpha)$ ratio is much smaller than the calculated values (~12%)[6] with realistic Stark mixing at $n = 3$. The result indicates either the initial sticking probability should be smaller (ω^0_s ~0.67%) or, if we believe the ω^0_s calculation, the atomic process of $(\alpha\mu)^+$ ions exhibiting in both R and γ_{K_α} has to be reconsidered to explain ω_s and $Y(K_\alpha)$ consistently. It is difficult to explain all the experimental data only by reducing initial sticking probability, and some enhancement of reactivation seems more probable.

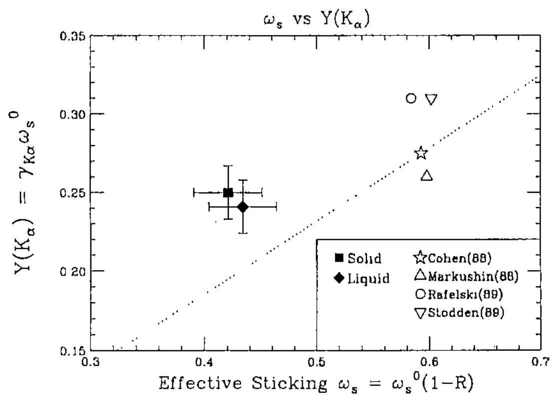

Fig. 7. The measured values of the effective sticking probability (ω_S) obtained from neutron data of the total loss rate and the K_α X-ray yield per fusion ($Y(K_\alpha)$). They are compared with the atomic process calculations by Cohen,[24] Markushin,[25] Rafelski,[26] and Stodden.[27] The values corresponding to $\omega^0_S = 0.912\%$ are shown by symbols.

In summary, we performed the first systematic measurements of the sticking X-ray and fusion neutron and the overall conclusions are as follows; the W and λ_c have, respectively, a minimum and a maximum at $C_t \sim 0.4$, while the W at $C_t \leq 0.2$ and ≥ 0.6 have a contribution from either dd or tt μCF; observed ω_s and $Y(K_\beta)/Y(K_\alpha)$ were both smaller than the theoretical predictions, while $Y(K_\alpha)$ was not contradicting with some of the theories. This result provides new constraints to the calculations of either initial sticking probability ω^0_s or the atomic process of $(\alpha\mu)^+$ in terms of γ_{K_α}, γ_{K_β} and R, and will lead to further understanding of the μCF.

The authors acknowledge contributions to the μCF facility construction by Drs. T. Hashimoto, H. Sugai, Messrs. P. Wright, R. Hall, D. Haynes, W. A. Morris, G. Thomas, and H. J. Jones. Contributions at the earlier stage of the μCF facility construction by Dr. H. Umezawa and Professor H. Kudo are also acknowledged. The authors would like to thank Professors A. Arima, M. Oda, Drs. P. Williams, A. D. Taylor and

W. G. Williams and others related persons at RIKEN and RAL for their kind supports and encouragements. Helpful discussions with Professor M. Kamimura and Dr. J. S. Cohen are also acknowledged.

References

1) W. H. Breunlich, P. Kammel, J. S. Cohen, and M. Leon: Ann. Rev. Nucl. Sci. **39**, 311 (1989).
2) L. I. Ponomarev: Contemp. Phys. **31**, 219 (1990).
3) K. Nagamine and M. Kamimura: Adv. Nucl. Phys. **24**, 151 (1998).
4) S. E. Jones et al.: Phys. Rev. Lett. **56**, 588 (1986).
5) W. H. Breunlich et al.: Phys. Rev. Lett. **58**, 329 (1987).
6) J. S. Cohen: Phys. Rev. Lett. **58**, 1407 (1987).
7) K. Nagamine et al.: Muon Catal. Fusion **5/6**, 289 (1990).
8) K. Nagamine, K. Ishida, S. Sakamoto, Y. Watanabe, and T. Matsuzaki: Hyperfine Interact. **82**, 343 (1993).
9) H. Bossy et al.: Phys. Rev. Lett. **59**, 2864 (1987).
10) K. Nagamine et al.: Hyperfine Interact. **101/102**, 521 (1996).
11) T. Matsuzaki et al.: to be submitted to Nucl. Instrum. Methods Phys. Res.
12) N. Kawamura: Ph.D. thesis, The University of Tokyo (1998).
13) S. N. Nakamura and M. Iwasaki: Nucl. Instrum. Methods Phys. Res. A **388**, 220 (1997).
14) S. E. Jones and A. N. Anderson: Proc. an International Symposium on Muon Catalyzed Fusion μCF-89, edited by J. D. Davies, RAL-90-022 (1990).
15) P. Ackerbauer et al.: Hyperfine Interact. **82**, 357 (1993).
16) V. M. Bystritskii et al.: Zh. Eksp. Teor. Fiz. **80**, 1700 (1981).
17) L. Bracci et al.: Phys. Lett. A **134**, 435 (1989).
18) N. Kawamura et al.: to be published.
19) P. E. Knowles et al.: Hyperfine Interact. **101/102**, 21 (1996).
20) D. L. Demin et al.: Hyperfine Interact. **101/102**, 13 (1996).
21) T. Matsuzaki et al.: RIKEN-RAL T_2-μCF experiment, to be published.
22) S. E. Jones, S. F. Taylor, and A. N. Anderson: Hyperfine Interact. **82**, 303 (1993).
23) C. Petitjean et al.: Hyperfine Interact. **82**, 273 (1993).
24) M. Struensee and J. S. Cohen: Phys. Rev. A **38**, 44 (1988).
25) V. E. Markushin: Muon Catal. Fusion **3**, 395 (1988).
26) H. E. Rafelski, B. Muller, J. Rafelski, D. Trautmann, and R. D. Viollier: Prog. Part. Nucl. Phys. **22**, 279 (1989).
27) C. D. Stodden, H. J. Monkhorst, K. Szalewicz, and T. G. Winter: Phys. Rev. A **41**, 1281 (1990).
28) Chi-Yu Hu, G. M. Hale, and J. S. Cohen: Phys. Rev. A **49**, 4481 (1994).